

***Herschel* and *Planck*: surprises in the sub-mm band**

Joaquín González-Nuevo González¹

¹ Inst. de Física de Cantabria (CSIC-UC), Avda. los Castros s/n, 39005 Santander, Spain

Abstract

This paper focused on three of the most spectacular and almost unexpected results obtained from the observations in the sub-mm band coming from the ESA's *Herschel* and *Planck* missions: the detection of hundred of strongly lensed galaxies, the identification of high- z proto-clusters, and the study of the weak lensing signal through the cross-correlation analysis. Although, there were theoretical works that anticipate them, none of these interesting results appeared in the original scientific programs of both mission. For this reason we have called them “surprises”.

1 Introduction

During the past years, the simultaneous operation of the ESA's *Herschel* [41] and *Planck* [42] missions has given us an unprecedented opportunity to cover one of the last few observational gaps in the far-infrared and sub-millimeter (sub-mm) regions of the electromagnetic spectrum. *Herschel* is an observatory facility that covers the 55 – 671 μm spectral range with angular resolution ranging between 6 and 35'' [41]. *Planck* is a surveyor that is observing the whole sky in nine spectral bands between 350 μm and 1 cm and with angular resolution ranging from ~ 4 to ~ 33 arcmin. *Planck* has two frequency channels close to *Herschel* bands: the 545 and 857 GHz (550 and 350 μm) High Frequency Instrument (HFI) channels.

The overlap in time and frequency between *Herschel* and *Planck* is not accidental: the two missions have been designed keeping in mind the added scientific value of a synergy between them. In addition to providing a broader spectral coverage of common sources, the combination of *Planck* and *Herschel* data will be beneficial in other respects. The much higher resolution and sensitivity of *Herschel* makes it well suited for follow-up of *Planck* sources, allowing to assess the effects of source confusion in *Planck* channels. In some cases it can be possible to resolve objects detected as individual sources by *Planck* into separated sources. More generally *Herschel* will make possible to quantify the boosting of *Planck* fluxes by the many faint sources within its beam. Moreover, *Herschel* data can be used

to improve the foreground characterization, thus helping to distinguish between genuine, possibly extragalactic, point sources and compact Galactic cirrus, and to provide more precise positions, essential for the source identification. This knowledge will be important for the interpretation of the all-sky *Planck* survey data.

In turn, *Herschel* will benefit from the absolute calibration of *Planck* fluxes which is better than 2% up to 353 GHz, where it is based on the CMB dipole, and $\simeq 7\%$ in the 2 highest frequency channels (545 and 857 GHz) where it is based on a comparison with COBE/FIRAS [44, 60]. For comparison, the overall photometric accuracy of the *Herschel*-SPIRE instrument is currently estimated as 15% [54].

Both satellites, and thanks also to their synergy, have revolutionised the sub-mm-science with almost unexpected results coming from their observations in the sub-mm band. This paper focuses on three of the most spectacular results: the detection of hundreds of strongly lensed galaxies, the identification of proto-clusters, and the study of the inhomogeneous distribution of matter thanks to the cross-correlation analysis of the weak lensing signal.

2 Identification of Strongly Lensed Galaxies (SLGs)

In the last decade, surveys at sub-mm wavelengths have revolutionized our understanding of the formation and evolution of galaxies by revealing an unexpected population of high-redshift, dust-obscured galaxies called sub-mm galaxies (SMGs) which are forming stars at a tremendous rate (i.e. $\text{SFR} \geq 1000 \text{ M}_{\odot} \text{ yr}^{-1}$; [5]). Data collected before the advent of the European Herschel Space Observatory (*Herschel*; [41]) and the South Pole Telescope (SPT, [10]), suggested that the number density of SMGs drops off abruptly at relatively bright sub-mm ux densities ($\sim 50 \text{ mJy}$ at $500 \mu\text{m}$), indicating a steep luminosity function and a strong cosmic evolution for this class of sources (e.g.[19]). Several authors have argued that the bright tail of the sub-mm number counts may contain a significant fraction of strongly-lensed SMGs [4, 40, 35, 39, 29].

Preliminary indications in support of such expectations has been provided by the first results of the SPT that found a surface density of bright SMGs well in excess of predictions of models that do not account for flux boosting due to gravitational lensing [56]. The *Herschel* Multi-tiered Extragalactic Survey (HerMES; [38]) and the *Herschel* Astrophysical Terahertz Large Area Survey (H-ATLAS; [13]) are wide-field surveys ($\sim 380 \text{ deg}^2$ and $\sim 550 \text{ deg}^2$, respectively) conducted by the *Herschel* satellite. Thanks to its sensitivity and frequency coverage both surveys have provided the large samples needed to probe the gravitational lensing scenario at sub-mm wavelengths. [36] used only the first $\sim 1/40$ of the final area of the H-ATLAS project and found that, of the 10 sources with flux density at $500 \mu\text{m}$ $F_{500\mu\text{m}} > 100 \text{ mJy}$, five were easily identified as blazars or local galaxies. The remaining five sources, with photometric signatures indicating high redshifts ($z > 1$), are all gravitationally lensed (see Fig. 1). [58] applied the same method to $\sim 100 \text{ deg}^2$ of HerMES data and confirmed nine of the 13 SLGs identified. Therefore, together both works have demonstrated that $> 80\%$ of candidates with $F_{500\mu\text{m}} > 100 \text{ mJy}$ are strongly-lensed galaxies (SLG). These results suggests that about ~ 150 such sources can be detected, with the same method, over the full H-ATLAS

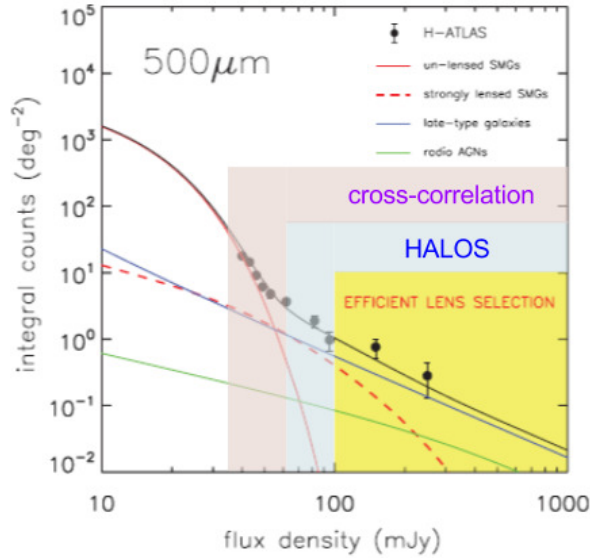


Figure 1: Description of the $\sim 100\%$ efficient SLGs selection procedure [36], compared with the HALOS methodology [17]. The cross-correlation analysis [18] makes use also of the faintest sources observed by the H-ATLAS survey.

area.

The first confirmed candidates, among the brightest ones, has been analysed in detail. In [8] the first ~ 30 candidates were confirmed and characterised. It was found that the lenses are at higher redshifts and have lower masses than lenses found in surveys based on optical spectroscopy, in agreement with expectations for a source-selected (rather than lens-selected) survey for lenses. In [12] the mass density radial profiles of the first five SLGs were obtained through lensing modelling. The results were consistent with other studies on the same topic, i.e. that the slope of the total mass density profile steepens with decreasing redshift and that the fraction of dark matter contained within half the effective radius increases with increasing effective radius and increases with redshift. Finally, [37] used the magnification factors estimated by [12] to derive the intrinsic properties of the lensed galaxies. This work concluded that these galaxies are thus proto-ellipticals caught during their major episode of star formation, and observed at the peak epoch ($z \sim 1.5 - 3$) of the cosmic star formation history of the Universe.

Moreover, strong gravitational lensing systems are powerful cosmographic probes and superb astronomical laboratories that can be exploited to study galaxy evolution over a wide range of redshifts (see [55] for a review on preliminary attempts). However, most of the strong lensing applications share a common limitation: the relatively small number of events to which they can be applied ([20] 20 SLGs; [50] 53 SLGs; [48] 11 SLGs, among others). At present there are about ~ 200 known SLGs. An increase by one order of magnitude in sample size is needed to make substantial progress in characterizing their emission, mass distribution and cosmological evolution properties, as well.

Driven by these previous results and sample size limitation, it was presented the HALOS (Herschel-ATLAS Lensed Object Selection, [17]) method a few years ago. This new strategy appeals to the fact that SLGs inevitably dominate the highest apparent luminosity tail of the high- z luminosity function and improve the selection efficiency of candidate SLGs fainter than $F_{500\mu\text{m}} > 100$ mJy by looking for close associations (within a few arcsec) with optical galaxies that may qualify as being the lenses. In [17], it was showed that this strategy can allow to reach candidate SLG surface densities of $\sim 1.5 - 2$ deg $^{-2}$, implying a total of ~ 1000 sub-mm SLGs in the full H-ATLAS survey (five times the present number of known SLGs). Such sample can become a game changer tool to understand the mass distribution and its cosmic evolution at galaxy scales (see Fig. 1).

Due to its particular characteristics (higher number of candidates, fainter sources, etc.) it was created a dedicated follow-up campaign, with observational time for tens of candidates on different instruments. Preliminary results confirm the validity of the method, although the final reliability have to be yet updated. On this respect, the first observational confirmation of one of the HALOS candidates has been recently submitted for publication [59]. By using near-infrared (near-IR) IFU spectroscopic observations it was detected a line, arc-like in shape, around the bulge of the lensing galaxy, in the H-band which was interpret as H α at $z = 1.46$, consistently with the far-infrared (far-IR) photometric redshift. By modelling the lensing system it was inferred a magnification factor of $\mu \sim 10$. The inferred (de-magnified) SFR is about $150 M_{\odot} \text{yr}^{-1}$, much lower than previous sub-mm-selected lensed galaxies, and more representative of the population of galaxies responsible for the cosmic star formation density at its peak. This result demonstrates the capability of the new method for studying strongly lensed galaxies at high redshift, with the potential of delivering several hundred new lensed galaxies, with the prospect of constraining the cosmological parameters and studying in detail the physical properties of normal star forming galaxies at high redshift.

3 Identification of proto-clusters

The discovery of distant far-IR luminous galaxies by sub-mm imagers (e.g. [26, 52]) and the discovery of the Cosmic Infrared Background [46, 14] have demonstrated the importance of the far-IR/sub-mm bands in determining a complete picture of the history of galaxy formation and evolution. The high redshift ($z \sim 2 - 3$) sources detected in these sub-mm surveys are expected to be the progenitors of the giant elliptical galaxies that we see today (e.g. [6]). In the framework of hierarchical clustering models of large scale structure and galaxy formation we would expect that the most massive elliptical galaxies form in the cores of what will become today's most massive galaxy clusters. [19] and others predict that multiple galaxies in such regions will undergo dust obscured starbursts at about the same time, producing clumps of dusty proto-spheroidal galaxies.

Hints of such objects may already have been found by clustering studies with Spitzer (e.g. [31]), or using high- z quasars as signposts for possible proto-clusters [53]. The latter study finds far more sub-mm bright companions to quasars than expected, implying the presence of dusty proto-clusters. Meanwhile, the highest redshift proto-cluster currently known, at $z \sim 5.3$, includes at least one sub-mm luminous object [9]. While this object is

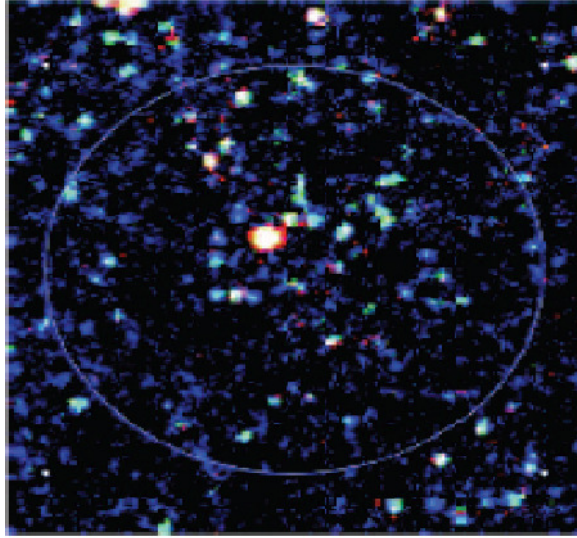


Figure 2: *Herschel* 3 colour image of region around HATLAS J114637.9-001132. Colours are: blue ($250\ \mu\text{m}$), green ($350\ \mu\text{m}$), and red ($500\ \mu\text{m}$). The colour scale has been chosen so that objects that are red/white are likely to lie at $z \sim 3$. The brightest white/red object in this image is the $z = 3.259$ lensed galaxy HATLAS J114637.9-001132 [15]. The light blue circle is centered on the *Planck* source and is the size of the *Planck* 857 GHz beam.

extreme, such sources may need to be quite common if the recent discovery of a mature galaxy cluster at $z = 2.07$ [16], with a fully formed red-sequence of galaxies with ages > 1.3 Gyr, is representative of a significant population.

The dusty star-forming phase of a proto-cluster is likely to be quite short, so the objects should be rare on the sky. Fortunately, *Herschel* and *Planck* are up to this challenge. *Herschel* allows relatively large areas of the sky to be covered to sensitive flux levels at wavelengths corresponding to the peak of the dust spectral energy distribution (SED) of high redshift starbursts (e.g. [36]). Meanwhile, *Planck* provides all sky coverage at wavelengths matching the longest *Herschel* bands and stretching into the sub-mm. Therefore, *Planck* can find cold compact structures and *Herschel* can then confirm that these are associated with clumps of galaxies, potentially at high redshift.

[34] examined the effect of clustering on the extragalactic sources that would be detected by instruments with large beams, such as the *Planck* High Frequency Instrument (HFI), which has an ~ 5 arcmin beam full width half-maximum (FWHM). They concluded that if the beam is approximately matched to the clustering scale, then the large beam instrument will detect the clustered sources as unresolved, or marginally resolved, discrete sources, and that these clusters will make a significant contribution to the source counts measured in such surveys. Now that the first data products from the *Planck* survey have been released, we can test these ideas by examining *Herschel* images of sources listed in the *Planck* Early Release Compact Source Catalog (ERCSC). Clusters of dusty star-forming galaxies along the lines of those proposed by [34] will appear as groups of discrete objects in the *Herschel* maps,

while contaminating sources, such as foreground, bright early-type galaxies or cirrus dust, will appear very different, respectively, as either single bright sources or extended diffuse emission.

[23] presented the results of a cross-correlation of the *Planck* ERCSC with the catalogue of *Herschel*-ATLAS sources detected in the phase 1 fields. There were 28 ERCSC sources detected by Planck at 857 GHz in this area. As many as 16 of them were high Galactic latitude cirrus; 10 additional sources can be clearly identified as bright, low- z galaxies; one further source is resolved by Herschel as two relatively bright sources; and the last is resolved into an unusual condensation of low-flux, probably high-redshift point sources, around a strongly lensed H-ATLAS source at $z = 3.26$ (see Fig. 2). These results demonstrate that the higher sensitivity and higher angular resolution H-ATLAS maps provide essential information for the interpretation of candidate sources extracted from *Planck* sub-mm maps.

The potential for *Planck* to detect clusters of dusty, star-forming galaxies at $z > 1$ was also tested in [11] by examining the *Herschel*-SPIRE images of *Planck* ERCSC sources lying in fields observed by the *Herschel* Multitiered Extragalactic Survey. Of the 16 Planck sources that lie in the 90 deg^2 examined, 12 were associated with single bright Herschel sources (local galaxies). The remaining four are associated with overdensities of *Herschel* sources, making them candidate clusters of dusty, star-forming galaxies. Complementary optical/near-IR data for these ‘clumps’ were used to test this idea, and find evidence for the presence of galaxy clusters in all four cases. Photometric redshifts and red sequence galaxies were used to estimate the redshifts of these clusters, finding that they range from 0.8 to 2.3. These redshifts imply that the *Herschel* sources in these clusters, which contribute to the detected *Planck* flux, are forming stars very rapidly, with typical total cluster star formation rates $> 1000 M_{\odot} \text{ yr}^{-1}$. The high-redshift clusters discovered in these observations are used to constrain the epoch of cluster galaxy formation, finding that the galaxies in these clusters are 1 – 1.5 Gyr old at $z \sim 1 - 2$.

Other studies using targeted observations of sources selected by their colours from the *Planck* maps, rather than the *Planck* catalogues used previously (Montier et al., in preparation), are also underway. Prospects for the discovery of further clusters of dusty galaxies are discussed, using not only all sky Planck surveys, but also deeper, smaller area, Herschel surveys.

4 Weak lensing through cross-correlation analysis

As photons from distant sources travel across the universe to reach our telescopes and detectors, their trajectories are perturbed by the inhomogeneous distribution of matter. Most sources appear to us slightly displaced and distorted in comparison with the way they would appear in a perfectly homogeneous and isotropic universe. This phenomenon is called weak gravitational lensing (e.g. [47], and references therein).

Furthermore, the deflection, on the one hand, stretches the area of a given sky region, thus decreasing the surface density of sources and, on the other hand, magnifies the background sources, increasing their chances of being included in a flux-limited sample. The

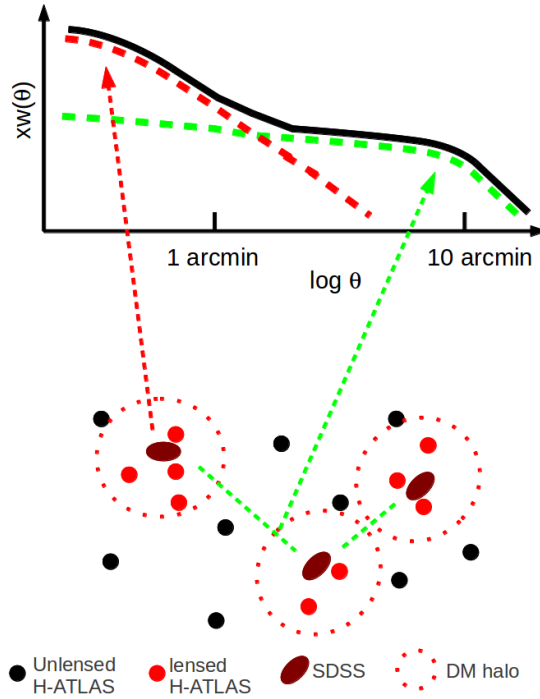


Figure 3: Interpretation diagram of the cross-correlation signal measured by [18].

net effect, termed magnification bias, is extensively described in the literature (e.g. [49]). It implies that an excess/decrease of background sources from a flux-limited sample will be found in the vicinity of matter overdensities [1, 33, 51]. The amplitude of the excess increases with the slope of the background source number counts. The most dramatic manifestations of lensing, called strong lensing, which includes multiple images, arcs or Einstein rings, show up on angular scales of arcseconds and provide information on high-density structures such as galaxies or galaxy clusters. The lower density structures, which include most of the mass in the Universe, nevertheless, can still produce observable effects via weak lensing.

The magnification bias due to weak lensing modifies the galaxy angular correlation function, because the observed images do not coincide with true source locations [21, 27, 33, 30], but the effect is generally small and difficult to single out. An unambiguous manifestation of weak lensing is the cross-correlation between two source samples with non-overlapping redshift distributions. The occurrence of such correlations has been tested and established in several contexts: 8σ detection of cosmic magnification from the galaxy–quasar cross-correlation function [51]; a simultaneous detection of gravitational magnification and dust reddening effects due to galactic haloes and large-scale structure (galaxy–quasar cross-correlation; [32]); and a 7σ detection of a cross-correlation signal between $z \sim 3 - 5$ Lyman-break galaxies and *Herschel* sources ([24]) among others. See also [2] and references therein.

A first attempt at measuring lensing-induced cross-correlations between *Herschel*/SPIRE galaxies and low- z galaxies was carried out by [57], who found convincing evidence of this

effect. More recently, it was reported a highly significant ($> 10\sigma$) spatial correlation between galaxies with $F_{350\mu\text{m}} \geq 30\text{ mJy}$ detected in the equatorial fields of the H-ATLAS with estimated redshifts 1.5, and Sloan Digital Sky Survey (SDSS) or Galaxy And Mass Assembly (GAMA) galaxies at $0.2 \leq z \leq 0.6$ [18]. The significance of the cross-correlation is much higher than those reported so far for samples with non-overlapping redshift distributions selected in other wavebands. Extensive, realistic simulations of clustered sub-mm galaxies amplified by foreground structures confirm that the cross-correlation can be explained by weak gravitational lensing ($\mu < 2$). The simulations also show that the measured amplitude and range of angular scales of the signal are larger than those that can be accounted for by galaxy–galaxy weak lensing. However, for scales < 2 arcmin, the signal can be reproduced if SDSS/GAMA galaxies act as signposts of galaxy groups/clusters with halo masses in the range $10^{13.2} - 10^{14.5} M_{\odot}$. The signal detected on larger scales appears to reflect the clustering of such haloes (see Fig. 3). Similar conclusions were obtained by [7] trying to explain that redder and brighter sub-mm sources have optical associations with a broader distribution of positional offsets than would be expected if these offsets were due to random positional errors in the source extraction. Such result has important consequences for counterpart identification and derived redshift distributions and luminosity functions of sub-mm surveys.

On the other hand, the CMB lensing potential is an integrated measure of the matter distribution in the Universe, up to the last-scattering surface. It has a broad kernel, peaking at $z \sim 2$ but slowly varying from $z = 1$ to $z = 4$. The study of cross-correlations with other tracers of large scale structure covering narrow redshift ranges allows us to reconstruct the dynamics and spatial distribution of the cosmological gravitational potentials. This can tighten tests of the time evolution of dark matter density fluctuations and through that give constraints on the dynamics of the dark energy at the onset of cosmic acceleration. Since the cross-correlations measure the average lensing signal from the dark matter halos that host the galaxies we can also derive from them the cosmic bias, hence the effective halo masses associated to the tracer populations. Although the bias factors can also be well determined from the auto-power spectra, we must always beware of unaccounted systematic effects. The cross-correlation measurements are not prone to systematics that are not correlated between the two datasets. Thus a comparison of the bias estimates from auto- and cross-correlations can uncover unforeseen systematics on either side.

Several catalogs, such as those from the NRAO VLA Sky Survey (NVSS), SDSS, the Wide Field Survey Infrared Explorer (WISE) have already been cross-correlated with the CMB lensing potential. These surveys cover large areas of the sky but detected sources are mostly at $z < 1$. The H-ATLAS allows to extend the cross-correlation analysis up to substantially higher redshifts [28, 17].

Highly statistically significant correlations between the CMB lensing and the Cosmic Infrared Background (CIB) have been recently reported [25, 22, 43, 45]. However, the CIB is an integrated quantity and the interpretation of the measured cross-correlations depend on the adopted redshift distribution of sources, derived from a model. The study of the cross-correlation carried by [3] with individually detected sources has the the double advantage that redshifts are estimated directly from the data and are distributed over a quite narrow range.

In that paper, it was presented the first measurement of the correlation between the map of the CMB lensing potential derived from the *Planck* nominal mission data and $z \geq 1.5$ galaxies detected by the H-ATLAS survey covering about 600 deg^2 , i.e. about 1.4% of the sky. The no CMB lensing-galaxy correlation hypothesis was rejected at a 20σ significance, checking the result by performing a number of null tests. The significance of the detection of the theoretically expected cross-correlation signal is found to be 8.2σ . The galaxy bias parameter, b , derived from a joint analysis of the cross-power spectrum and of the auto-power spectrum of the galaxy density contrast is found to be $b = 2.80_{-0.11}^{+0.12}$, consistent with earlier estimates for H-ATLAS galaxies at similar redshifts. On the other hand, the amplitude of the cross-correlation is found to be a factor 1.62 ± 0.16 higher than expected from the standard model and also found by cross-correlation analyses with other tracers of the large-scale structure. The enhancement due to lensing magnification can account for only a fraction of the excess cross-correlation signal. It was suggested that most of it may be due to an incomplete removal of the contamination of the CIB, that includes the H-ATLAS sources we are cross-correlating with. In any case, the highly significant detection reported here using a catalogue covering only 1.4% of the sky demonstrates the potential of CMB lensing correlations with sub-mm surveys.

5 Conclusions

As usual in science, the unexpected results became the most interested ones. In fact, the three topics presented here have opened three new research lines that are very promising for the understanding of galaxy formation, dark matter or dark energy among other interesting applications.

Acknowledgments

JGN acknowledges financial support from the Spanish CSIC for a JAE-DOC fellowship, co-funded by the European Social Fund. The work has been supported in part by the Spanish Ministerio de Ciencia e Innovación, AYA2012-39475-C02-01, and Consolider Ingenio 2010, CSD2010-00064, projects.

References

- [1] Bartelmann, M. & Schneider, P., 1993, *A&A*, 268, 1
- [2] Bartelmann, M. & Schneider, P., 2001, *Physics Reports*, 340, 291
- [3] Bianchini, F. et al. 2015, *ApJ*, accepted
- [4] Blain, A. W. 1996, *MNRAS*, 283, 1340
- [5] Blain, A. W., et al. 1999, *MNRAS*, 309, 715
- [6] Blain, A. W., et al. 2002, *Physics Reports*, 369, 111
- [7] Bourne, N. et al., 2014, *MNRAS*, 444, 1884

- [8] Bussmann, R. S. et al., 2013, *ApJ*, 779, 25
- [9] Capak, P. L., et al. 2011, *Nature*, 470, 233
- [10] Carlstrom, J.E., et al. 2011, *PASP*, 123, 568
- [11] Clements, D. L., et al. 2014, *MNRAS*, 439, 1193
- [12] Dye, S. et al., 2014, *MNRAS*, 440, 2013
- [13] Eales, S., et al. 2010, *PASP*, 122, 499
- [14] Fixsen, D. J., et al. 1998, *ApJ*, 508, 123
- [15] Fu, H., et al. 2012, *ApJ*, 753, 134
- [16] Gobat, R., et al. 2011, *A&A*, 526, A133
- [17] Gonzalez-Nuevo, J., et al. 2012, *ApJ*, 749, 65
- [18] Gonzalez-Nuevo, J., et al. 2014, *MNRAS*, 442, 2680
- [19] Granato, G. L., et al. 2004, *ApJ*, 600, 580
- [20] Grillo, C., et al. 2008, *A&A*, 477, 397
- [21] Gunn, J. E., 1967, *ApJ*, 147, 61
- [22] Hanson, D., et al. 2013, *PhRvL*, 111, 141301
- [23] Herranz, D., et al. 2013, *A&A*, 549, A31
- [24] Hildebrandt, H. et al., 2013, *MNRAS*, 429, 3230
- [25] Holder, G. P., et al. 2013, *ApJL*, 771, L16
- [26] Hughes, D. H., et al. 1998, *Nature*, 394, 241
- [27] Kaiser, N. 1992, *ApJ*, 388, 272
- [28] Lapi, A., et al. 2011, *ApJ*, 742, 24
- [29] Lima, M., et al. 2010, *MNRAS*, 406, 2352
- [30] Loverde, M. et al., 2008, *PhRevD*, 77, 023512
- [31] Magliocchetti, M., et al. 2007, *MNRAS*, 375, 1121
- [32] Menard, B. et al., 2010, *MNRAS*, 405, 1025
- [33] Moessner, R. & Jain, B. 1998, *MNRAS*, 294, L18
- [34] Negrello, M., et al. 2005, *MNRAS*, 358, 869
- [35] Negrello, M., et al. 2007, *MNRAS*, 377, 1557
- [36] Negrello, M., et al. 2010, *Science*, 330, 800
- [37] Negrello, M. et al., 2014, *MNRAS*, 440, 1999
- [38] Oliver, S. J., et al. 2010, *A&A*, 518, L21
- [39] Paciga, G., et al. 2009, *MNRAS*, 395, 1153
- [40] Perrotta, F., et al. 2003, *MNRAS*, 338, 623
- [41] Pilbratt, G. L., et al. 2010, *A&A*, 518, L1

- [42] Planck Collaboration 2011, *A&A*, 536, A1
- [43] Planck Collaboration 2013, *A&A*, 571, A18
- [44] Planck HFI Core Team 2011, *A&A*, 536, A4
- [45] POLARBEAR Collaboration 2014, *PhRvL*, 112, 131302
- [46] Puget, J.-L., et al. 1996, *A&A*, 308, L5
- [47] Refregier, A. 2003, *ARA&A*, 41, 645
- [48] Ruff, A.J., et al., 2011, *ApJ*, 727, 96
- [49] Schneider, P. et al., 1992, *Gravitational Lenses*, XIV, 560 pp
- [50] Schwab, J., et al., 2010, *ApJ*, 708, 750
- [51] Scranton, R. et al., 2005, *ApJ*, 633, 589
- [52] Smail, I., Ivison, R. J. & Blain, A. W. 1997, *ApJL*, 490, L5
- [53] Stevens, J. A., et al. 2010, *MNRAS*, 405, 2623
- [54] Swinyard, B. M., et al. 2010, *A&A*, 518, L4
- [55] Treu, T. 2010, *ARA&A*, 48, 87
- [56] Vieira, J. D., et al. 2010, *ApJ*, 719, 763
- [57] Wang, L. et al., 2011, *MNRAS*, 414, 596
- [58] Wardlow, J. L., et al. 2013, *ApJ*, 762, 59
- [59] Williams, R. J., et al. 2014, *MNRAS*, submitted
- [60] Zacchei, A., et al. 2011, *A&A*, 536, A5